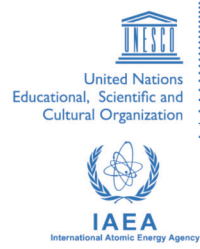




**The Abdus Salam
International Centre for Theoretical Physics**



SMR/1845-4

**Conference on Structure and Dynamics in Soft Matter and
Biomolecules: From Single Molecules to Ensembles**

4 - 8 June 2007

Direct Observations of Amyloid Fibril Growth and Propagation

Y. GOTO

*Institute for Protein Research
Osaka University
3-2 Yamadaoka, Suita
565-0871 Osaka
JAPAN*

Direct Observation of Amyloid Fibril Growth and Propagation

Yuji Goto

Institute for Protein Research, Osaka University, Japan; E-mail: ygoto@protein.osaka-u.ac.jp

Amyloid fibrils form through nucleation and growth. To clarify the mechanism involved, direct observations of both processes are important (1, 2). First, seed-dependent fibril growth of β 2-microglobulin (β 2-m) and amyloid β peptide was visualized in real-time at the single fibril level using total internal reflection fluorescence microscopy combined with the binding of thioflavin T, an amyloid-specific fluorescence dye (3-5). Second, using atomic force microscopy, ultrasonication-induced formation of β 2-m fibrils was shown, indicating that ultrasonication is useful to accelerate the nucleation process (6). Third, with the proteolytic fragment of β 2-m, propagation and a transformation of fibril morphology was demonstrated (7). These direct observations indicate that template-dependent growth and structural diversity are key factors determining the structure and function of amyloid fibrils.

References

1. Ban, T. *et al.* (2006) *Acc. Chem. Res.* **39**, 663-670.
2. Chatani & Goto (2005) *Biochim. Biophys. Acta* **1753**, 64-75.
3. Ban, T. *et al.* (2003) *J. Biol. Chem.* **278**, 16462-16465.
4. Ban, T. *et al.* (2004) *J. Mol. Biol.* **344**, 757-767.
5. Ban, T. *et al.* (2006) *J. Biol. Chem.* **281**, 33677-33683.
6. Ohhashi, Y. *et al.* (2005) *J. Biol. Chem.* **280**, 32843-32848.
7. Yamaguchi, K. *et al.* (2005) *J. Mol. Biol.* **352**, 952-960.

1. Seed-Dependent Amyloid Fibril Growth

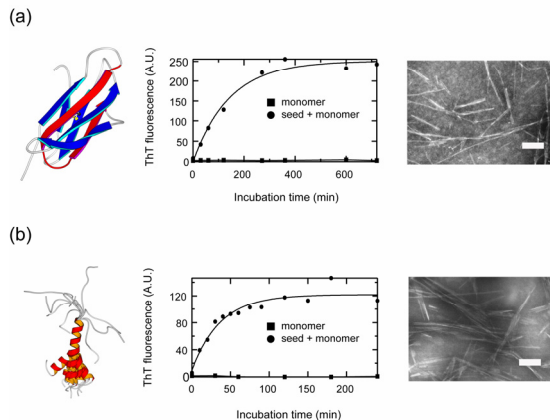


Fig. 1. Formation of amyloid fibrils of β 2-m (a) and A β (1-40) (b). (a) Three-dimensional representation of monomeric β 2-m (left) in the native state (PDB entry 1HSB). The location of K3 peptide is indicated by red. The time course of seed-dependent growth of amyloid fibrils of β 2-m at pH 2.5 as monitored by the increase in ThT fluorescence (center). Electron microscopic images of β 2-m fibrils obtained by the seed-dependent extension (right). (b) Three-dimensional representation of monomeric A β (1-40) (left) in a water-micelle environment. (PDB entry 1BA4). The time course of seed-dependent growth of amyloid fibrils of A β (1-40) at pH 7.5 (center). Electron microscopic images of A β (1-40) fibrils prepared by the seed-dependent extension (right). Scale bars represent 200 nm.

2. Total Internal Reflection Fluorescence Microscopy

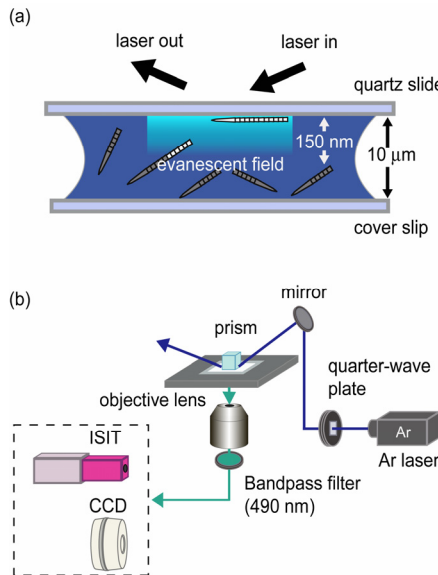


Fig. 2. Schematic representation of amyloid fibrils revealed by total internal reflection fluorescence microscopy. (a) The penetration depth of the evanescent field formed by the total internal reflection of laser light is \sim 150 nm for a laser light at 455 nm, so that only amyloid fibrils lying in parallel with the slide glass surface were observed. (b) Schematic diagram of a prism-type TIRFM system on an inverted microscope.

3. Real-Time Observation of Fibril Growth

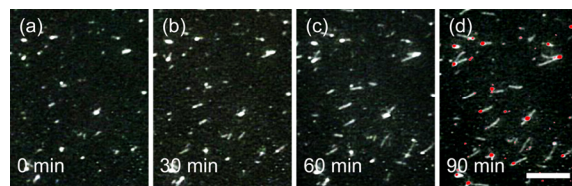


Fig. 3. Direct observation of β 2-m amyloid fibril growth obtained by TIRFM. The scale bars are 10 μ m. In the panel of 90 min, ThT fluorescence at 0 min was overlaid in red to identify the locations of seed fibrils.

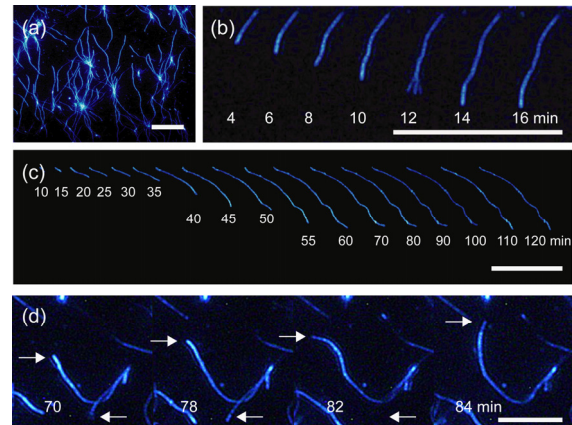


Fig. 4. Direct observation of A β (1-40) amyloid fibril growth by TIRFM. (a-i) Real-time monitoring of fibril growth on glass slides. Arrows indicate the unidirectional growth of A β from a single seed fibril. The scale bar represents 10 μ m.

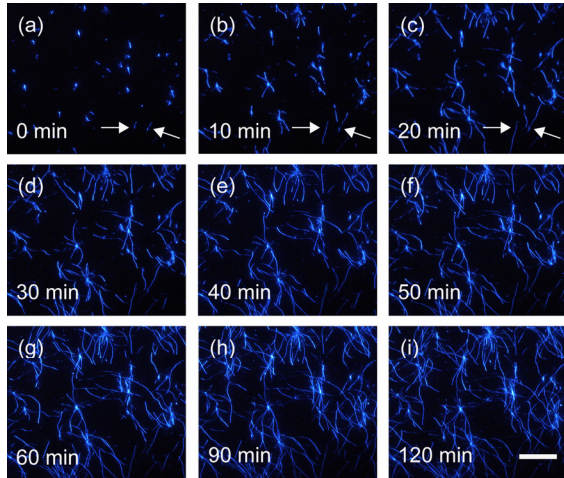


Fig. 5. Characteristic images of $\text{A}\beta(1-40)$ amyloid fibril growth revealed by TIRFM. (a) Vertically aligned image of fibrils. (b) Growth with transient fraying of the growing end at 12 min. (c) Growth with a swinging head producing a rugged fibril. The scale bars in (a-c) are 10 μm . (d) Growth with flexible bending motion. Top and bottom arrows indicate the bending horizontal and vertical, respectively, to the plane of the quartz surface. The scale bar represents 5 μm .

4. Ultrasonication-Induced Formation of Fibrils

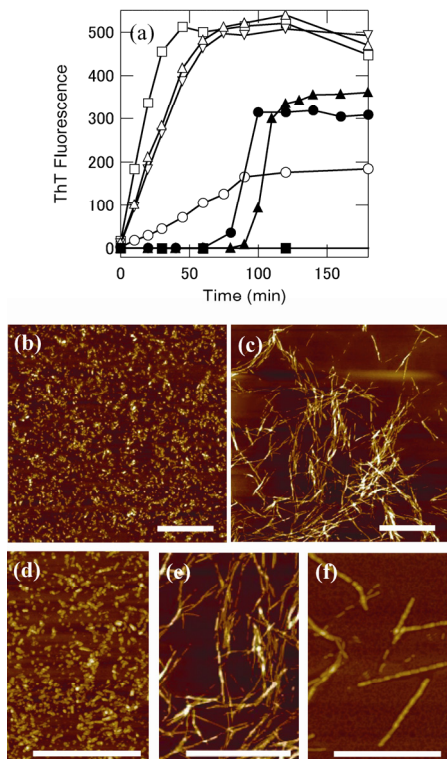


Fig. 6. Ultrasonication-induced formation of $\beta 2\text{-m}$ fibrils at pH 2.5. (a) Kinetics monitored by ThT fluorescence. (\bullet , \blacktriangle) Ultrasonication-induced formation of F1 fibril exhibiting a lag-time (60 - 120 min). The results of two independent experiments are shown, indicating a slight variation of lag-time. (\square , Δ , ∇) Extension reaction producing F2 (\square), F3 (Δ), and F4 (∇) fibrils, in which ultrasonication-induced F1, F2, and F3 fibrils were used as seeds, respectively. (\circ), Standard fibril extension reaction with seeds of originally *ex vivo* $\beta 2\text{-m}$ amyloid fibrils. (\blacksquare), Control reaction without seeds and ultrasonication. (b-f) AFM images of F1 (b, d) and F2 (c, e) fibrils and fibrils extended by the standard reaction at pH 2.5 (f). The scale bars represent 1 μm .

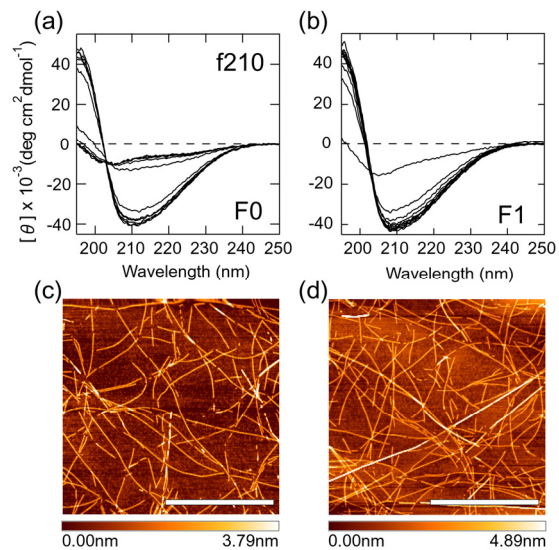


Fig. 7. Seeding-dependent propagation of f210 fibrils. (a, b) CD spectra of f210 fibrils prepared by spontaneous polymerization (F0) (a) and by seeding of f210 fibrils (F1) (b) in 20% (v/v) TFE and 10 mM HCl at 25 °C. (c, d) AFM images of F0 (c) and F1 (d) f210 fibrils.

5. Inheritance versus Adaptation of Fibril Conformation

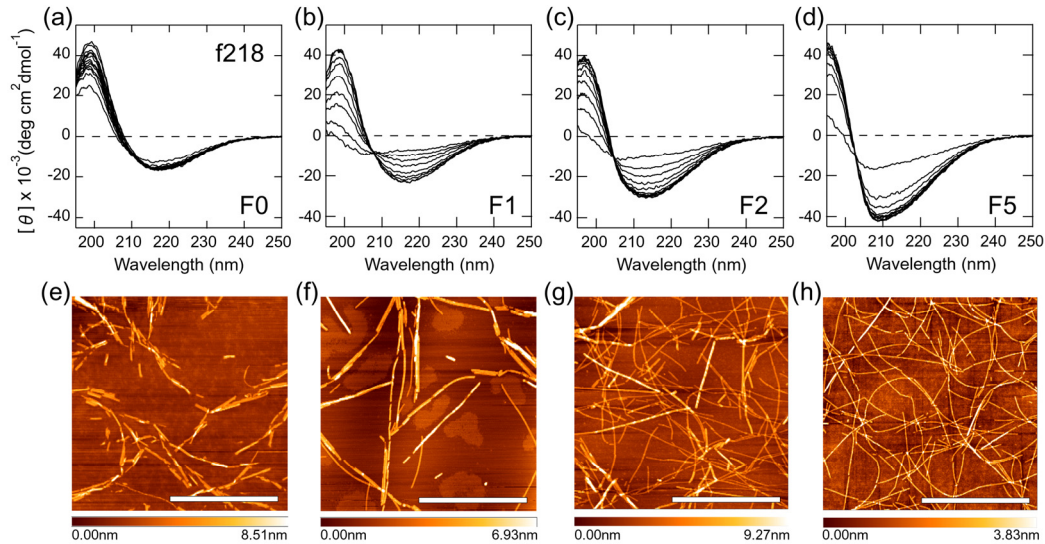


Fig. 8. Transformation of f218 fibrils into f210 fibrils during the repeated cycles of self-seeding. (a-d) Seed-dependent formation of fibrils in 20% (v/v) TFE and 10 mM HCl at 25 °C monitored by CD. Types of fibrils made were F0 (a), F1 (b), F2 (c), and F5 (d). (e-f) AFM images of F0 (e), F1 (f), F2 (g), and F5 (h) fibrils.

7. Free Energy Landscapes Illustrating Fibril Formation, Propagation, and Adaptation

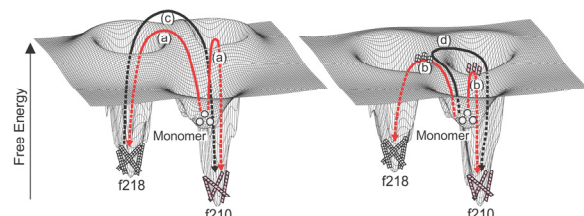


Fig. 9. Schematic representation of energy landscapes for the formation of f210 and f218 fibrils in the absence (left) and presence (right) of seeds. (a) Spontaneous formation of f210 and f218 fibrils with a high free energy barrier. (b) Seed-dependent formation of f210 and f218 fibrils with a reduced free energy barrier. Starting with f218 fibrils contaminated with a small amount of f210 fibrils, the repeated-seeding reaction increases the population of f210 fibrils leading to conformational adaptation. (c) Conformational adaptation by the direct conversion of f218 fibrils to f210 fibrils through the free energy barrier separating them. The conversion can also occur through the monomers in equilibrium with the two types of amyloid fibrils. (d) Conformational adaptation during the growth of single fibrils, where f218 seeds are used to initiate the reaction but the peptides assume a thermodynamically stable f210 conformation.